4-2018

Interference of the Inflammasome Via Interferonβ

Madeline Sauer
University of Dayton

Interference of the Inflammasome Via Interferonβ

Honors Thesis

Madeline Sauer

Department: Health and Sports Science

Advisor: Joel D. Schilling, M.D., Ph.D. and Anne Crecelius, Ph.D.

April 2018

Interference of the Inflammasome Via Interferonβ

Honors Thesis

Madeline A. Sauer

Department: Health and Sports Science

Advisor: Joel D. Schilling, M.D., Ph.D. and Anne Crecelius, Ph.D.

April 2018

Abstract

Metabolic disorders such as type two diabetes mellitus (T2DM) and obesity are known to have a chronic low grade inflammatory tissue environment as well as an increase in excess lipids. Current research suggests that a tightly regulated oligoprotein complex known as the NLRP3 inflammasome is highly activated in T2DM and obesity. However, it is not well understood the interplay between excess lipids, which was previously shown in our lab to cause lysosome damage, and inflammation. A key transcription factor that is known to have both an inflammatory effect as well as an effect on lipid metabolism is PPARγ. For this reason, we attempted to determine if PPARγ had an effect on the degree of pro-inflammatory cytokine release such as IL-1β in the presence of excess lipids. A myeloid specific knock-out of PPARγ (mPPARγ KO) showed significantly less IL-1β and IL-1α levels when stimulated with palmitate-LPS. The selective suppression of the IL-1 family occurred via transcriptional changes. RNA sequencing data showed that the mPPARγ KO had a heightened type 1 IFN signature, with both increases in IFNβ and IFN-regulated genes. The type-1 interferon receptor antibody (IFNAR1 ab) raised IL-1 levels to wild type levels, confirming the PPARγ phenotype was due to the heightened IFNβ levels. When WT macrophages were stimulated with palm-LPS and recombinant IFNβ (rIFNβ), it phenocopied the mPPARγ KO macrophages, confirming IFNβ was sufficient to decrease IL-1 levels. These findings suggest crosstalk between lipid metabolism and inflammation in macrophages, adding to the understanding of the complex pathology seen in T2DM and obesity.

Acknowledgements

I would like to thank my mentor, Dr. Joel Schilling, M.D., Ph.D. for his support during this project. I am very grateful for his patients, motivation and immense knowledge during this project. I would also like to thank the whole Schilling lab for their help with this project, specifically Gowri Kalugotla and Li He. I would like to thank Washington University School of Medicine for their facilities. I would like to thank the NIH for the two grants that made this project possible: NIH RO1 DK11003401 and NIH P30 DK020579. I would like to thank my on-campus advisor Dr. Anne Crecelius, Ph.D. as well. She helped immensely with coordinating between Washington University and the University of Dayton. Lastly, I would like to thank the University of Dayton Honors Department for their help and support during this project.

UNIVERSITY of DAYTON

Table of Contents

Introduction

Type two diabetes mellitus (T2DM) is a chronic metabolic disorder that has become increasingly common in the United States and around the world. According to the American Diabetes Association, in 2015 almost 10% of the American population had T2DM which is 30.3 million Americans (1). Since 1953, the CDC reports over a fivefold increase in the number of individuals with diabetes, as seen in the Figure on the right (2). As the prevalence of T2DM and obesity, which is also a chronic metabolic disorder often associated with T2DM, continue to skyrocket health care costs to manage these difficult diseases continue to increase accordingly. Diabetes is the seventh leading cause of death among Americans and is likely higher due to many diabetes complications related deaths.

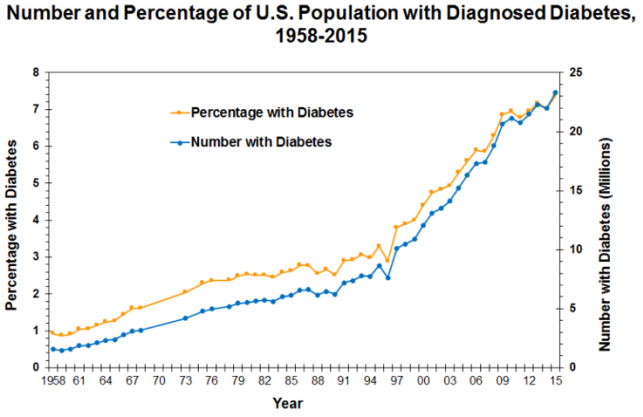

The hallmark of T2DM is insulin resistance, which is often monitored clinically with hemoglobin A1c (HbA1c) levels. However, blood glucose levels are not the only clinically relevant pathology associated with T2DM. Typically, T2DM presents with an excess in circulating free fatty acids (FFAs) and triglycerides, as well as excess lipid accumulation in tissues (3, 4). It is known that T2DM also has metabolic and inflammatory phenotypes which adds to the complexity of the disease. The immune system is known to be altered in the adipose tissue of patients with T2DM, as well in other tissues such as the liver (5). Despite the knowledge that both metabolism and inflammation play a key role in the pathology of T2DM, their interplay is not well understood. Therefore, it is advantageous for this reason to study the metabolic and inflammatory differences that are seen in patients with T2DM, to determine possible treatments.

Specifically within T2DM, there are changes in lipid update and metabolism which can lead to the metabolic and inflammatory phenotypes seen. A high lipid environment causes an increase in lipid update from macrophages which can lead to a pro-inflammatory phenotype (6, 7). It is this low grade, but persistent inflammation that are related to the many complications of diabetes. When excess lipid is taken up by macrophages in conjunction with another stress signal, such as tissue damage from a pathogen or ischemia, the macrophage can be propelled into activation of an inflammatory response. This other stress signal needed can come in a variety of flavors such as lipopolysaccharide (LPS), silica, viral infection, double stranded DNA (dsNDA) and cholesterol

signals. It is when both excess lipid is present, as well as the other stress signal that an oligoprotein complex known as the NLRP3 inflammasome can become activated (8). The inflammasome is a tightly regulated inflammatory complex which leads to a pro-inflammatory phenotype due to release of certain cytokines (9, 10). The schematic below shows this concept.

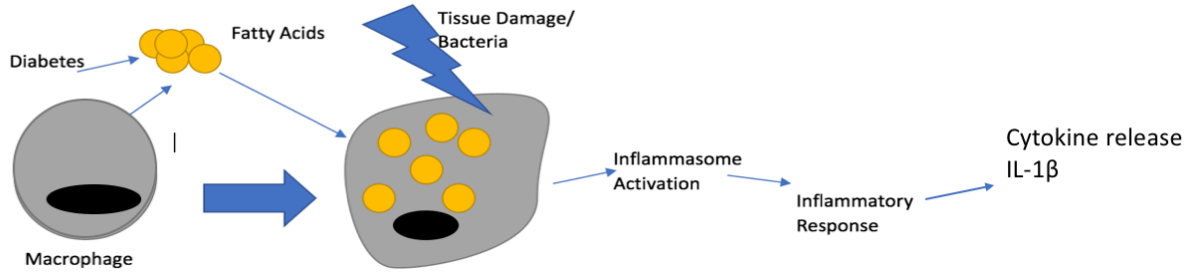

The inflammasome activation will cause an inflammatory response, which has read outs of cytokine release, such as interluken-1 (IL-1) and tumor necrosis factor alpha (TNFα). The pro-inflammatory cytokine IL-1β specifically is a hallmark cytokine secreted when the inflammasome is fully activated. IL-1 levels have been shown to be strongly associated with risk of T2DM and atherosclerosis in both animal and human models (11-14). Since the NLRP3 inflammasome requires two signals, namely signal 1 which is propagated through TLRs, and signal 2 which is from excess fatty acids leading to lysosome damage (8, 15). TLRs are critical innate immune receptors that respond to pathogens or tissue damage which provides the first priming signal for the inflammasome complex. The excess lipid environment was shown in our lab to lead to lysosome damage, which activates signal 2, leading to the fully formed and activated inflammasome (6). It is important to note that one signal is not sufficient to activate the complex, but when both danger signals are present, the inflammasome can become active.

Since it is known that both the high lipid environment and lysosome damage through signal 2 are needed for the inflammasome complex to be active, we wanted to establish a mode which would mimic the T2DM environment and lead to activation of both signals. Palmitate, which is an 18-carbon chain fatty acid that is high concentrations in patients with T2DM was the source of signal 2 leading to lysosome damage (5, 6, 16). LPS, which is an endotoxin, was given as the source of signal 1 leading to TLR4 activation. Signal 1 is mediated through activation of a toll-like receptor (TLR), which is an innate immune receptor on the cell surface, by a ligand (17, 18). This leads to activation of NF-κB and

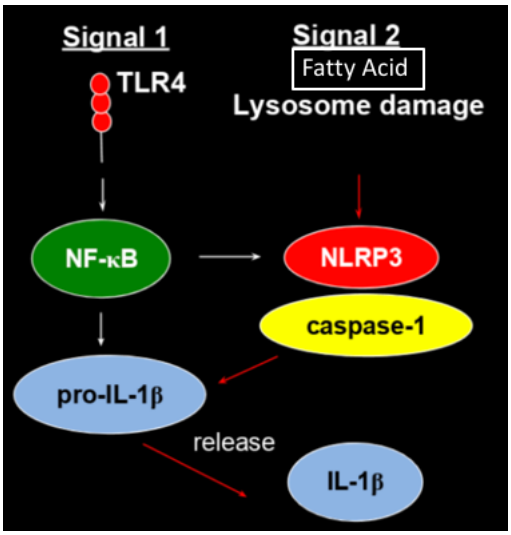

upregulation of transcripts such as NLRP3 and pro-IL-1β. The second signal, in our lab the palmitate, stimulates the assembly of the inflammasome complex, and allows for caspase-1 to cleave pro-IL-1β (18, 19). This allow for the release of mature IL-1β which is biologically active and can lead to pro-inflammatory effects. Without both signals mature IL-1β cannot be released (5, 17). Since the different signals lead to distinct activation of different parts of the inflammasome complex, that can be used as markers to determine what changes are arising from different treatments or cell lines.

It was of interest to our lab to better understand the mechanism by which a high lipid environment can lead to excess inflammation in macrophages and determine the interplay between inflammation and metabolism, since these are hallmark pathologies associate with T2DM. For this reason, a transcription factor called peroxisome proliferator-activated receptors-gamma (PPARγ) became of interest to us. PPARγ is in a class of nuclear receptors and is expressed in immune cells such as primary macrophages (20). PPARγ is known to affect lipid modulation and it aids in fatty acid update which was established earlier in this paper to lead to inflammasome activation (18, 21). Current research supports that PPARγ has largely an anti-inflammatory role, since activation of PPARγ leads to down-regulation of pro-inflammatory cytokines such as iNOS and TNF-α (20). Agonists of PPARγ are currently used therapeutically for patients with T2DM, due to data that showed loss of PPARγ from obesity models of macrophages led to increased insulin resistance (22, 23). However, agonists of PPARγ use in humans is controversial due to cardiovascular complications.

Based on this prior data, we hypothesized that PPARγ would suppress inflammasome activation, and understanding its mechanism of action could provide insight into the interplay between lipid metabolism and inflammation in macrophages. Therefore, we also hypothesized that loss of PPARγ from primary macrophages would heighten inflammasome activity and increase pro-inflammatory cytokines synthesis and release. This study investigated a myeloid specific knock-out of PPARγ mouse model (mPPARγ KO) to test this hypothesis. Interestingly, we found that loss of PPARγ from myeloid cells stimulated with palmitate and LPS to activate the NLRP3 inflammasome led to selective decrease in IL-1β and IL-1α release. This selective decrease in IL-1 levels occurred due to mRNA regulation which led to decrease in the production of pro-IL-1β and pro-IL-1α protein. RNA sequencing showed a heightening type 1 interferon (IFN) response via upregulation of type 1 IFN genes in the stimulated mPPARγ KO macrophages. IFNβ, a type 1 IFN cytokine, was both necessary and sufficient to lead to the selective reduction in IL-1 levels in stimulated cells. Our lab confirmed these finding via qPCR analyzing mRNA levels of IFNβ regulated genes. When IFNβ signaling was blocked by the addition of the type 1 interferon receptor

(IFNAR1) antibody, IL-1 levels were normalized to wild type (WT) levels. Furthermore, when WT macrophages were treated with recombinant IFNβ (rIFNβ), it led to selective reduction in IL-1 levels, phenocopying the mPPARγ KO cells. When a synthetic ligand of PPARγ, rosiglitazone, was given it lead to suppression of IFNβ and IFN-regulated genes. A prior study showed similar results that activation of PPARγ led to negative regulation of IFNβ production (20). This data suggests that loss of PPARγ from primary macrophages leads to heightened IFNβ production, which leads to suppression of the transcription of IL-1 levels. It is important to know that this data is currently part of a larger project in which the manuscript is currently under review to be published in the Journal of Immunology (24).

Methods

Reagents- L-NIL was from Enzo life sciences (Farmingdale, NY, USA). T0070907 was from TOCRIS (Minneapolis, MN, USA). Rosiglitazone and α-tubulin antibody were from Sigma Chemical (St. Louis, MO, USA). IL-1β, IL-1α, NLRP3, STAT1 and phospho-STAT1(#14994) antibodies were from Cell Signaling (Danvers, MA, USA). IFNβ and the IFNβ ELISA were from PBL (Piscataway, NJ, USA). The PE conjugated α-IFNAR antibody were from Biolegend (San Diego, CA, USA). IFNAR blocking antibody (MAR1-5AE) and control IgG were from Leinco Technologies (St. Louis, MO, USA). Duoset ELISA kits (IL-1β, IL-1α, TNFα) were from R&D Systems (Minneapolis, MN, USA). Ultrapure E. coli LPS and silica were from Invivogen (San Diego, CA, USA). Thioglycollate was from Difco-BD (Franklin Lakes, NJ, USA). Fatty acids were from Nu-Chek Prep (Waterville, MN, USA). Ultrapure-bovine serum albumin (BSA) was from Lampire (Ottsville, PA, USA) and was tested for TLR ligand contamination prior to use by treating primary macrophages and assaying for TNFα release. Full list of reagents used for the manuscript available (manuscript in preparation) (24).

Cell Culture- Peritoneal macrophages (pMACs) are resident macrophages that are recruited in response to intraperitoneal injection of 3.58% sterile thioglycollate. Macrophages were isolated from C57BL/6, or the indicated knockout mice. Four days after injection the pMACs are then isolated using an 18 gauge needle. Cells were plated at a density of 1.0 X 10^6 cells/mL in Dulbecco's modified Eagle's medium containing 10% inactive fetal serum (IFS), 2mM L-glutamine, 50 U/mL penicillin G sodium, 50U/mL streptomycin sulfate (pen-strep), and 1mM sodium pyruvate. When indicated medium was supplemented with 500 μM palmitate. Fatty acid supplemented medium was prepared by modification of the method of Spector. Briefly, a 20 mM solution of fatty acid in 0.01 M NaOH was incubated at 70 °C for 30 min. Dropwise addition of 1 N NaOH facilitated solubilization of the fatty acid. Fatty acid soaps were complexed with 5% fatty acid-free BSA in phosphate-buffered saline at an 8:1 fatty acid to BSA molar ratio. The complexed fatty acid was added to the serum-containing cell culture medium to achieve a fatty acid concentration of 500 μM. The final fatty acid concentration in the medium was measured using a semimicroanalysis kit (Wako Chemicals). The final BSA concentration was measured using the Albumin Reagent (BCG, Sigma). The pH of the medium did not differ significantly with the addition of complexed fatty acid. This growth medium protocol was first described according to Ory and Schaffer lab (16). Stimulation of cells with palmitate and LPS were performed on the day after harvest. Peritoneal cells were plated on low adherence plates (Greiner Bio-One) for flow

cytometry experiments. Peritoneal cells were plated on a high adherence plate for RNA and protein experiments (Falcon). Cells used for flow cytometry were washed and removed from the plate with PBS, then 10 minutes with Cell Stripper (Gibco) and then 10 minutes with EDTA/trypsin (Sigma). Cells used for RT-qPCR were washed and removed from the plate with PBS on ice, then RNase free lysate buffer. Cells used for western blot were washed and removed from the plate with PBS on ice, then protease buffer was added and cells were gently scraped. BSA-supplemented medium was used as a control. For cell stimulations, PBS or LPS (100 ng/mL) were added to BSA or palmitate-containing medium. For triggering the NLRP3 inflammasome by non-lipid activators pMACs were treated with LPS 100 ng/ml for 16h after which they were incubated with vehicle, rIFNβ, or rosiglitazone.

Stimulations- There were four main types of stimulation performed during the experiments in this lab. To mimic the pro-inflammatory and excess lipid environment, the PL condition was used of palmitate and LPS (100ng/mL). The other treatments served as a control to compare when only signal 1 or 2 are given. PP condition contains the palmitate signal but uses PBS as a control to LPS. The BL conditions contain the LPS signal, but BSA is used as a control to palmitate. Finally, the BP condition contains both controls, namely BSA and PBS. It is important to note that only the PL condition contains both signals necessary to activate the inflammasome fully. After pMACs were allowed to adhere to the plate for 24 hours, the stimulation medial was made and added to cells. Stimulation media was left on cells for 22+ hours for ELISA, 8-16hrs for RNA, or 4-16hrs for protein.

Interferon Receptor Antibody with Stimulations- Peritoneal macrophages were isolated and stimulated with BSA-PBS or palmitate-LPS according to protocol above. Cells were pre-stimulated with IFNAR1 antibody in DMEM for 24hrs in concentration. Then IFNAR1 antibody was added to PL media, or the same volume of vehicle to serve as a control for 8 hours. Cells were then washed with PBS, then ice cold lysis buffer was added.

Recombinant IFN with Stimulations- Peritoneal macrophages were isolated and stimulated with BSA-PBS or palmitate-LPS according to protocol above. Cells were pre-stimulated with rIFNβ in DMEM overnight (~16hrs) in desired concentrations (either 25units, 50U, or 100U) or vehicle for control. Then the desired concentration of rIFNβ was added to PL media, or the same volume of vehicle to serve as a control for 1hr. Cells were then washed with PBS, then ice cold lysis buffer was added.

Rosiglitazone with Stimulations- Peritoneal macrophages were isolated and stimulated with BSA-PBS or palmitate-LPS according to protocol above. Cells were pre-stimulated with rosiglitazone at desired concentration (either 1μM or 10μM) in DMEM or vehicle as control overnight (~16hrs). Then macrophages were treated with PL media with the desired concentration of rosiglitazone or the same volume of vehicle to serve as a control for 8 hours. Cells were then washed with PBS, then ice cold lysis buffer was added.

Mice- Wild type (WT) C57BL/6 mice were bred in our mouse facility at Washington University School of Medicine. PPARγflox x LysM-Cre mice and LysM-Cre control mice were from Gwen Randolph (Washington University) and bred in our facility; IFNR1flox x LysM-Cre were from Mike Diamond (Washington University). All lines were in the C57BL/6 background. Mice were maintained in a pathogen-free facility on a standard chow diet *ad libitum* (6% fat). All animal experiments were conducted in strict accordance with National Institutes of Health guidelines for humane treatment of animals and were reviewed by the Animal Studies Committee of Washington University School of Medicine.

LysM-Cre Knock-out- The myeloid specific PPARγ knock-out (mPPARγ KO) was created using a LysM-Cre technology. This allowed us to selectively deplete PPARγ sequence from myeloid cells. Cre is the DNA recombinase that binds to the LoxP sequence. LoxP sequence was inserted in myeloid cells flanking each side of the PPARγ gene. LysM allows for the expression of Cre, making it macrophage specific. The Cre binds to the LoxP promoters, flanking the PPARγ gene, and causes the removal of the PPARγ sequence.

RNA Isolation, Quantitative RT-PCR and RNA sequencing- Total cellular RNA was isolated using Qiagen RNeasy column and reverse-transcribed using a high capacity cDNA reverse transcription kit (Applied Biosystems). Real-time qRT-PCR was performed using SYBR green reagent (Applied Biosystems) on an ABI 7500 Fast thermocycler. Relative gene expression was determined using Δ-Δ CT method normalized to 36B4 expression. Mouse primers sequence were as follows (all are 5' to 3'): ***36B4*** (forward, ATC CCT GAC CCG CCG TGA, reverse TGG GAG TAG ACA CAA GGT ACA ACC C); ***IL-1β*** (forward, AGG GAG AAC CAA GCA ACG ACA AAA; reverse, TGG GGA ACT CTG CAG ACT CAA ACT); ***NLRP3*** (forward; AAA ATG CCT TGG GAG ACT CA; reverse AAG TAA GGC CGG AAT TCA CC; ***CXCL10*** (forward; ATC ATC CCT GCG AGC CTA TCC TG; reverse, CGG ATT CAG ACA TCT CTG CTC ATC). ***TNFα*** (forward, 5′-CAT

CTT CTC AAA ATT CGA GTG ACA A-3′, reverse, 5′-TGG GAG TAG ACA CAA GGT ACA ACC C-3′); ***IFNβ*** (forward, 5′-GAC GGA GAA GAT GCA GAA GAG TT-3′, reverse, 5′-AGT TCA TCC AGG AGA CGT ACA AC-3′); ***IL-1α*** (forward- TGA GTT TTG GTG TTT CTG GC, reverse- TCG GGA GGA GAC GAC TCT AA); ***iNOS*** (forward- ACA TCG ACC CGT CCA CAG TAT, reverse- CAG AGG GGT AGG CTT GTC TC); ***MX1*** (forward- CCA GGT CCT GCT CCA CAC, reverse- TCT GAG GAG AGC CAG ACG AT).

The total cellular RNA was also prepared for RNA sequencing with the Clonetech SMARTer kit according to manufacturer's protocols, ligated with adapters and unique molecular indexes for each sample for every read, and then sequenced on one single-end 50bp lane on an Illumina HiSeq 3000. Full information on RNA-seq data available in manuscript (24).

Western Blotting- Total cellular protein was isolated by lysing cells in 150 mM NaCl, 10mM Tris (pH 8), Triton X-100 1% and 1 X Complete protease inhibitor (Thermo-Fisher Scientific). Proteins were separated on a TGX gradient gel (4-12%, Bio-Rad) for approximately 30 minutes. Proteins were then transferred from the gel to a nitrocellulose membrane. Protein was transferred overnight at 4 degrees C with constant amps. Western blotting for pro-IL-1β and tubulin was performed using 40μg of total cellular protein. The indicated primary antibody was diluted to desired concentration in milk in PBS and allowed to sit overnight at 4 degrees C. The next morning indicated secondary antibody was diluted to desired concentration in reagent diluent (1% BSA in PBS) was allowed to sit for 2+ hours at room temperature. Strips were washed between antibodies with PBS. Strips were developed with developing solutions per manufactures instructions and read in a BioRad machine. Tubulin was used a loading control.

IL-1β ELISA- Supernatants were harvested from macrophage culture after 24 hr stimulations. IL-1β, IL-1α and TNFα were quantified using a DuoSet ELISA kit (R&D Systems) according to manufacturer's instructions. A 96 well plate was coated overnight at room temperature with 100μL capture antibody with an analyte-specific antibody. The next morning the plate was washed with wash buffer (3x in PBS + 1% Tween). Then blocking buffer (reagent diluent, 1% BSA in PBS filtered) was allowed to sit on the plate for 2+ hrs in room temperature. The plate was then washed with wash buffer. Supernatants samples were diluted 1:2 in DMEM and a standard curve was then plated. Standard curve samples were created with a standard recombinant analyte in a 7 point standard curve using 2-fold serial dilutions in DMEM. Standard curve ranged from 1000 pg/mL to 15.6 pg/mL, and just DMEM served at the 8th standard curve point of 0 pg/mL so that any trace fluoresce from the DMEM was accounted for. Samples were allowed to incubate at room

temperature for 2+ hours. The plate was then washed with wash buffer. The plate was then coated in 100µL detection antibody for 2+ hrs. The plate was then washed with wash buffer. 100µL of working dilution of Streptavidin-HRP was then added to each well for 20 minutes in the dark at room temperature. 100µL of Substrate solution was then added to each well and allowed to incubate at room temperature in the dark for 20 minutes. 50µL of Stop Solution was then added to each well and gently mixed. The plate was then analyzed immediately for its optical density in a microplate reader set to 450 nm with a wavelength correction of 540nm to 570nm. Sample concentrations were compared to standard curve to determine optical density level. All antibodies were diluted from stock concentrations in reagent diluent (1% BSA in PBS filtered).

IFNR1 Flow Cytometry- Peritoneal macrophages were removed from low adherence plate and 1 x 106 cells were pelleted in FACS buffer (PBS, 1%BSA) and incubated with Fc block x 5 min on ice followed by incubation with IFNR1-PE (1:200) for 30 minutes on ice in the dark. Samples were analyzed on a FACS caliber flow cytometer (BD).

LDH Release Assay- After stimulations, macrophage supernatants were collected at 24 hrs, LDH was quantified using the CytoTox 96 non-radioactive cytotoxicity assay (Promega) per the manufacturer's instructions using a Tecan Infinite M200 per reader. Total LDH content was determined using the lysis buffer provided by the manufacturer. Prior studies in our lab (unpublished data) has shown there is no significant differences in LDH levels between WT and KO cells, indicating KO cells are not dying at a fast rate than WT cells.

IFNR1 Flow Cytometry- After the indicated stimulations, pMACs were removed from the low adherence plates as described above. 1 X 10^6 cells were pelleted in PBS and 1%BSA (FACS buffer) and incubated with Fc block for 5 minutes on ice followed by incubation with IFNR-PE (1:200) for 30 minutes on ice in the dark. Samples were analyzed on a FACS caliber flow cytometer (BD).

Statistics- Statistical analysis was performed using GraphPad Prism software. All the results are expressed as means ± S.E. Groups were prepared by paired Student's t-test or two way analysis of variance as appropriate. A value of $p \leq 0.05$ was considered significant.

Results

Myeloid Specific PPARγ Knock-out Mice Show Decreased IL-1 Levels

To gain a better understanding about what PPARγ was doing in macrophages, our lab created a myeloid specific PPARγ knock-out mouse. The hope of this model was to determine how lipid metabolism regulates inflammasome activation. First, we wanted to establish that in fact our mode was a myeloid specific knock-out. Figure 1A shows a western blot of our knock-out mouse, determining that in fact it was a true knock-out. The knock-out was also previously established in prior work in our lab (8, 25).

Peritoneal macrophages were elicited from WT and mPPARγ KO mice to study how they responded to the T2DM mimicked environment. The cells were bathed in palmitate or stearate and LPS for 8 hours or with BSA and vehicle. The stimulation protocol showed a significant decrease in IL-1β levels in the mPPARγ KO mice as compared with WT mice (Figure 1 B). Similarly, there was a reduction in the IL-1α , another pro-inflammatory cytokine of the IL-1 family (Figure 1C). This was shown to be selective for IL-1β, since TNFα was unchanged, and trended higher in the mPPARγ KO mice (Figure 1D). The unchanged TNFα levels indicates that knocking out PPARγ did not cause a global inflammasome defect or derangement of the innate immune receptor needed to signal inflammasome activation. This was also shown in our lab to be true in-vivo (data not shown). WT and mPPARγ KO mice were injected with LPS, then IL-1β, TNFα, IL-1α were measured in the peritoneal fluid 16 hours post LPS injection.

Figure 1

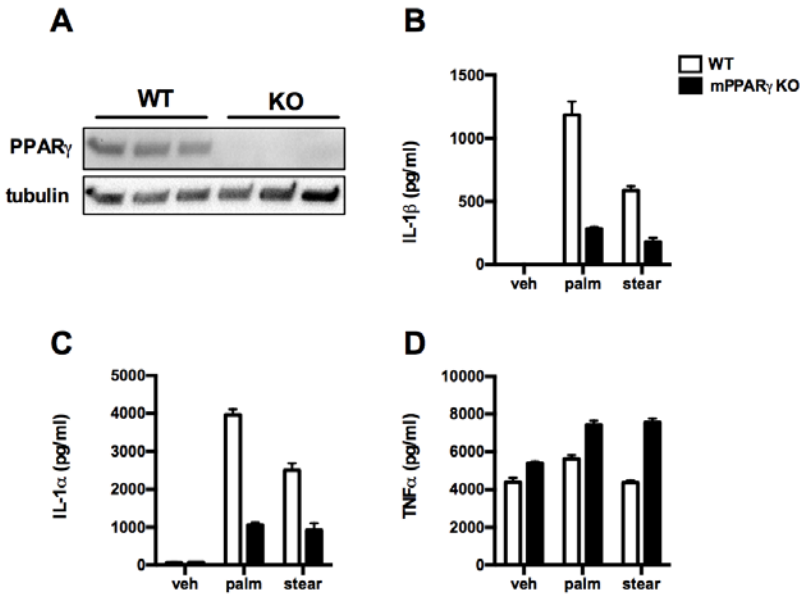

Figure 1. Myeloid Specific PPARγ Knock-out Mice Show Decreased IL-1 Levels. (**A**) Protein from peritoneal macrophages (pMACs) isolated from WT or mPPARγ KO mice were analyzed via western blot. (**B-D**) pMACs isolated from WT (open bars) or mPPARγKO mice (filled bars) were treated with vehicle (BSA-LPS), palm (250 μM)-LPS (100 ng), or stearate (150 μM)-LPS for 20hrs and the release of IL-1β (**B**), (**C**) IL-1α, and (**D**) TNFα was determined by ELISA.

IL-1 Levels Decrease Due to Signal 1 Effect on the Inflammasome

Once we determined that there was a specific inhibition of IL-1 levels when mPPARγ KO cells were treated with PL, we wanted to determine what part of the inflammasome complex was being effected. More specifically, we wanted to determine if the effect was specifically on IL-1β transcription, translation, or release, or if it was due to something upstream in the inflammasome such as an effect on NLRP3. The inflammasome complex must receive both signal 1 and signal 2 to have release of the mature IL-1β. Pro-IL-1β is a product of signal 1 activation and is necessary to get mature IL-1β cleavage from caspase-1 (26). At the protein level, there was also shown to be a difference in pro-IL-1β or pro-IL-1α (Figure 2A). When examining NLRP3, there were no differences at the mRNA level, but instead was selectively decreasing IL-1β and IL-1α mRNA (Figure 2B). This data suggests that all of the necessary machinery is present within these KO cells, there is just a selective inhibition of IL-1. Since the pro-IL-1 protein is affected, this indicates that PPARγ deficiency is causing a transcriptional change in the signal 1 effect on the inflammasome leading to the decreased IL-1 levels seen in our KO model. When a kinetic analysis of pMACs in PL from 0-16 hrs was performed, there was proportional reduction in IL-1β mRNA levels (Figure 2C). When TNFα mRNA was measured, there was no difference between the genotypes (Figure 2D).

Figure 2

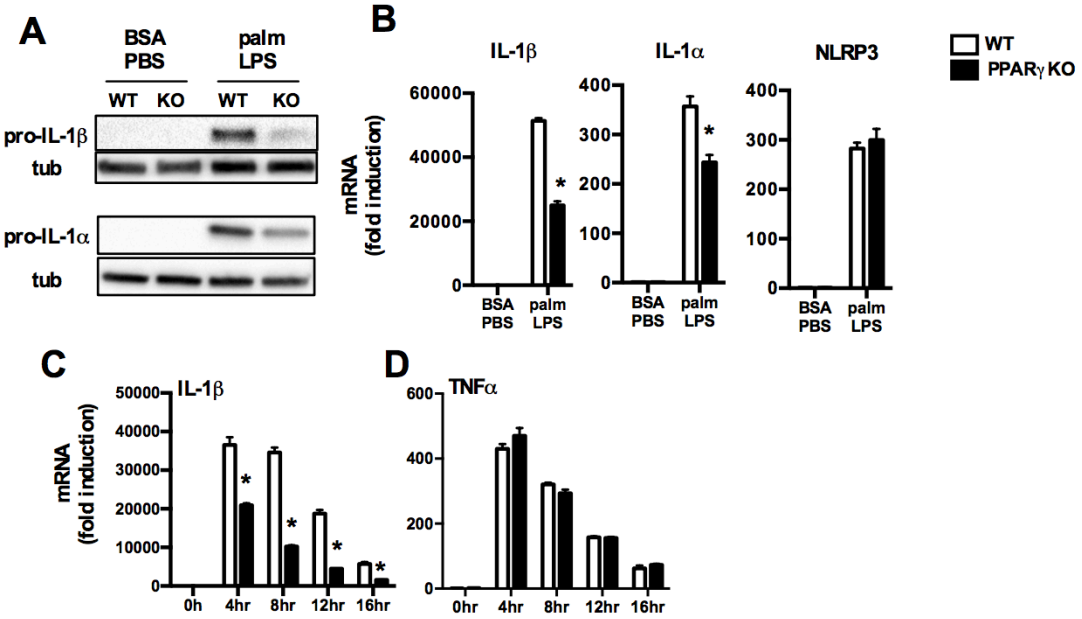

Figure 2. IL-1 Levels Decrease Due to Signal 1 Effect on the Inflammasome. (**A**) WT or mPPARγKO (KO) macrophages were stimulated with BSA-PBS (vehicle) or palm-LPS for 16hrs and the protein level of pro-IL-1β and pro-IL-1α was assessed by western blotting. Tubulin (tub) is shown as a loading control. (**B**) pMACs isolated from WT (open bars) or mPPARγKO mice (filled bars) were treated with vehicle or palm-LPS for 8hrs and mRNA expression of IL-1β, IL-1α, and NLRP3 was assessed by qRT-PCR. (**C, D**) Kinetic assessment of IL-1β (**C**) and TNFα (**D**) mRNA levels following palm-LPS stimulation in WT and mPPARγKO cells. Bar graphs report the mean ± standard error (SE) for a minimum of 3 experiments, each performed in triplicate. *, $p<0.05$ for WT vs. mPPARγKO or; ns, non-significant.

RNA Sequencing of Myeloid Specific PPARγ Knock-out Mice Reveals Enhanced IFNβ Pathways

Since PPARγ is a transcription factor, next we wanted to perform RNA sequencing on the cells since RNA sequencing is an unbiased quantitative method to determine all the transcripts present within a cell. The RNA sequencing data was useful for us to determine if any biological pathways of relevance in the WT versus the KO cells. Cells were treated under four different conditions: BSA and PBS (BP), BSA and LPS (BL), palmitate and LPS (PL) and palmitate and PBS (PP). Figure 3 compares the WT to the KO cells, highlighting the biggest differences between the two cell lines, with a cutoff of a 2.0-fold change in gene expression. The top 20 upregulated pathways in the mPPARγ KO versus the WT pMACs are show in Figure 3A. Interestingly, one of

the biggest readouts was differences in the IFNβ pathway. The boxed hits indicate pathways that are associated with the innate immune response and interferonβ (IFNβ). Figure 3B shows the top 10 differences between the KO and WT cells for biological processes. Note that 6 of the top 10 are related to IFNβ production or response. Figure 3C is a heatmap representing differences in gene expression *in the response to IFNβ* module shows consistent increases in gene expression for IFNβ and IFN target genes in the KO cells. Blue indicates lower gene expression, whereas the red indicates higher gene expression. There is an increase in almost all of the IFNβ related genes in the KO cells compared with the WT mice under the PL treatment.

Figure 3

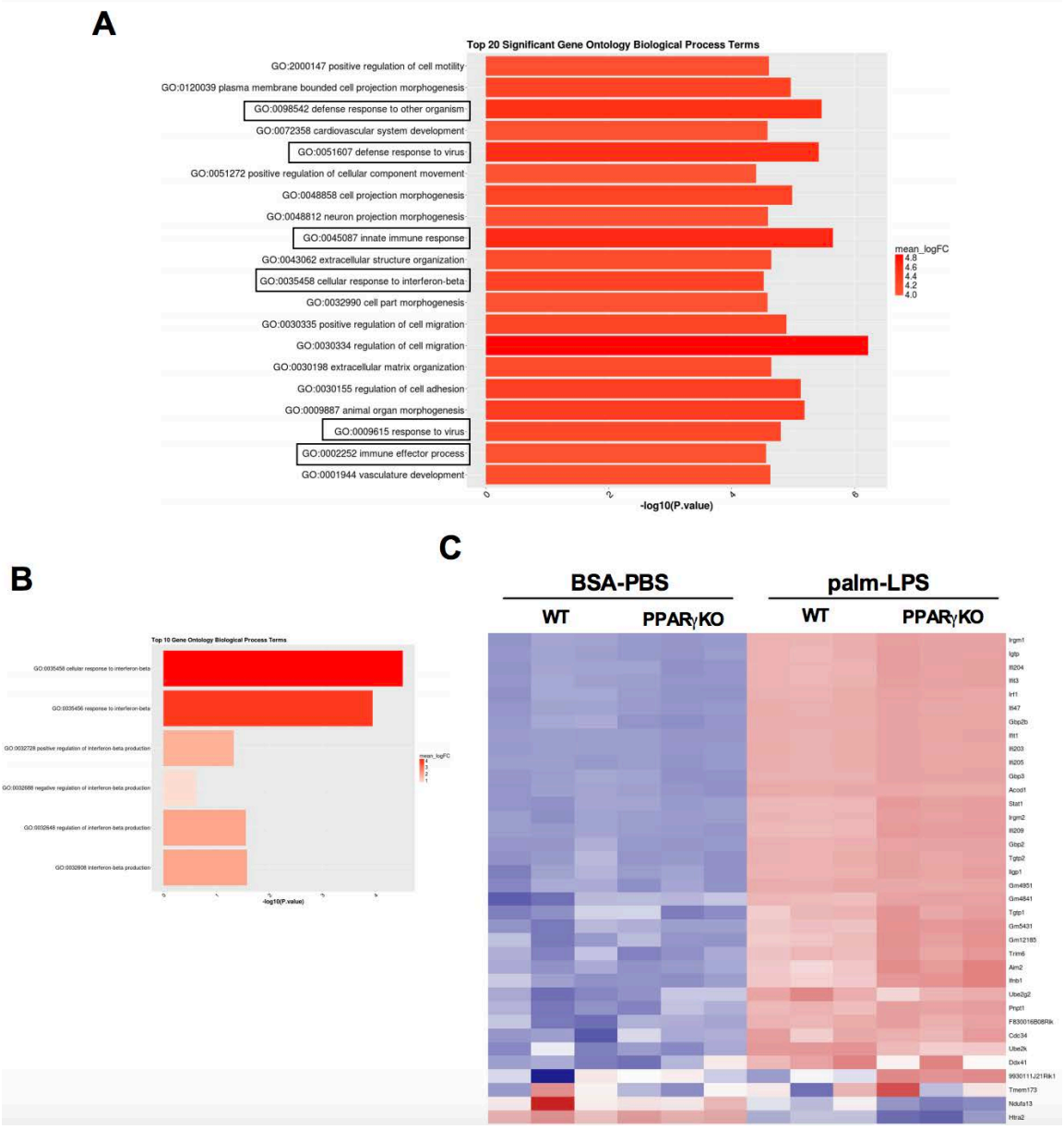

Figure 3. RNA Sequencing of Myeloid Specific PPARγ Knock-out Mice Reveals Enhanced IFNβ Pathways. (**A-C**) WT or PPARγKO pMACs were treated with BSA-PBS or palm-LPS for 8hrs after which RNA was isolated and RNA sequencing was performed. (**A**) Pathway analysis of the top 20 upregulated biologic processes in PPARγKO compared to WT pMACs treated with palm-LPS. Biologic pathways related to innate host defense are shown in the boxes. (**B**) Group summary for pathways related to IFNβ in PPARg vs. WT pMACS treated with LPS. (**C**) Heatmap expression profile of genes from the cellular response to IFNβ GO biologic processes module. WT and PPARγKO cells are shown under basal conditions (BSA-PBS) and after activation (palm-LPS).

Stimulated Myeloid Specific PPARγ Deficient Macrophages Have Heightened IFNβ Expression and Release

To confirm this in our lab, we performed qPCR on the mPPARγ KO and WT pMACs analyzing type 1 interferon gene targets including MX1, and CXCL10. MX1 and CXCL10 are IFN-regulated genes, so act as biomarkers to measure IFNβ activity (27). At the mRNA level, there was a significant increase in both IFN-regulated genes (Figure 4A). At the protein level, phoso-STAT1 was then analyzed in the KO cells treated with PL when compared with the WT (Figure 4B). IFNβ, a type-1 interferon, signals through the type 1 interferon receptor (IFNAR1), which is known to lead to phosphorylation of STAT (28). STAT1 is a transcription factor which then can drive gene expression of IFN-dependent genes. Western blot showed an increase in STAT1 phosphorylation in the mPPARγ KO cells compared to the WT (Figure 4B). To note in Figure 4C, there is no differences in the interferon receptor density between the WT and KO cells, as analyzed via flow cytometry. This indicates that the differences seen in the IFN related genes and IFNβ levels is due to changes in transcription or release, and not due to an increase density in its receptor. We then analyzed IFNβ levels in the WT versus the KO cells at both an mRNA level and in cytokine release via ELISA. Figure 4D and E shows that the KO cells have about a 2 fold increase in the amount of IFNβ at both the mRNA and release level. This indicates that there is an increase in transcription of IFNβ as well as in the release of mature IFNβ. This data indicates that the mPPARγ KO cells have a heightened IFNβ response.

Figure 4

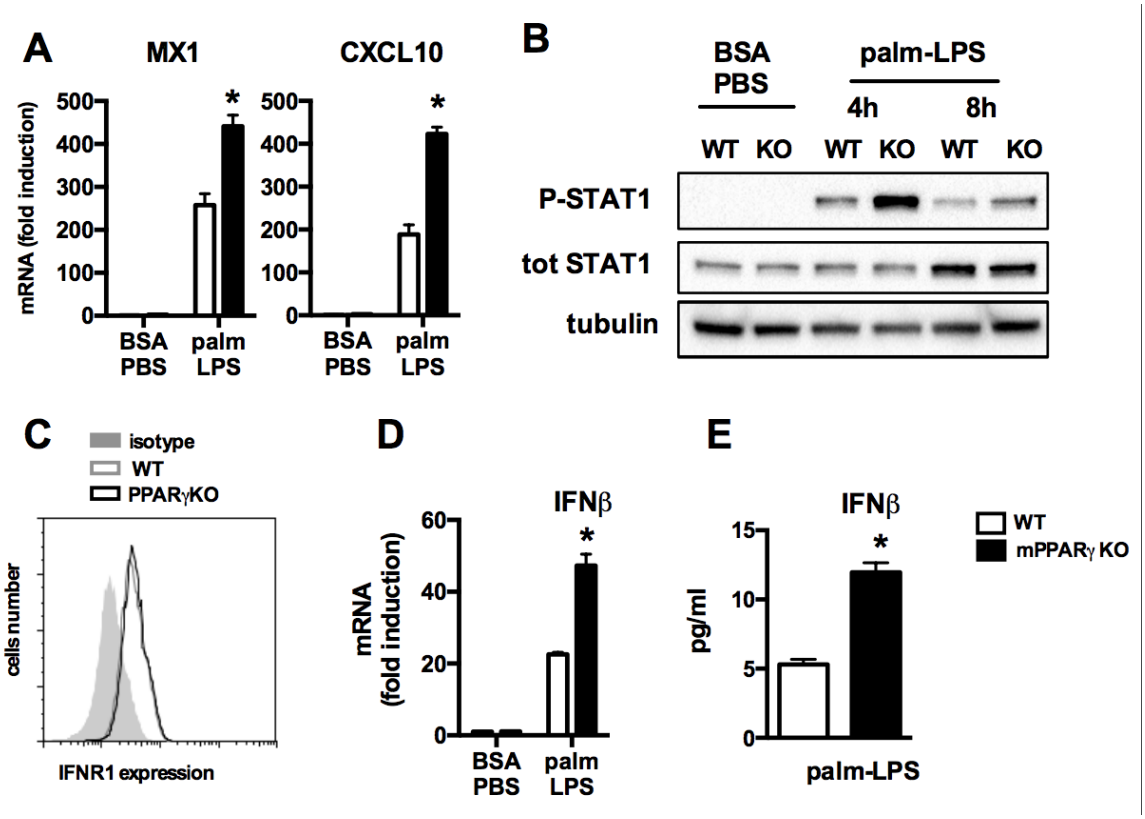

Figure 4. Stimulated Myeloid Specific PPARγ Deficient Macrophages Have Heightened IFNβ Expression and Release. (**A**) pMACs isolated from WT (open bars) or mPPARγKO mice (filled bars) were treated with vehicle or palm-LPS for 8hrs and mRNA expression of MX1 and CXCL10 targets was determined by qRT-PCR. (**B**) Macrophages were treated with vehicle or palm-LPS for 4hrs or 8hrs after which cell lysates were isolated and phopho(P)-STAT1 (Y701) was assessed by western blotting. Total (tot) STAT1 and tubulin are shown as controls. (**C**) pMACs from WT or PPARγ KO mice were stained with an antibody the type 1 interferon receptor (IFNAR) and receptor surface expression was assessed by flow cytometry and is shown as a representative histogram. (**D**) mRNA levels of IFNβ were quantified in WT and mPPARγKO cells at 1hr after palm-LPS treatment via qRT-PCR. (**D**) IFNβ release from WT and KO pMACs 6hrs after palm-LPS stimulation via ELISA. Bar graphs report the mean ± standard error (SE) for a minimum of 3 experiments, each performed in triplicate. *, $p<0.05$ for WT vs. mPPARγKO; ns, non-significant

Neutralization of the IFNβ Signal Normalizes IL-1 Levels in Myeloid Specific PPARγ Knock-out Mice

Next we wanted to determine if the heightened IFNβ response was a possible mechanism for the selective inhibition of IL-1 in the mPPARγ KO mice. To determine if IFNβ is necessary for the IL-1 response, we treated WT and the KO pMACs in the PL condition with a control IgG or the interferon receptor (IFNAR) antibody. IFNβ must go through the IFNAR1 receptor to enter into the pMACs and cause any cellular changes. The data showed that when the KO cells were treated with the IFNAR antibody returned the IL-1β levels to the WT baseline (Figure 5A). Note there was a decrease in the IL-1β levels when cells were treated with the control IgG, which is consistent with our previous data. It is also important to note that treatment with the IFNAR1 antibody led to a modest increase IL-1β levels in WT cells when compared with vehicle stimulation, which provides further evidence that IFNβ may be leading to the decreased IL-1 levels seen in the mPPARγ KO (Figure 5A). T0070907 is a known PPARγ antagonist. Cells were pre-stimulated with T0070907 for 24hrs then stimulations were performed as specified in the methods. When T0070907 was given to WT cells it led to a decrease in IL-1β levels compared to WT cells treated with vehicle, which further confirmed that PPARγ was required for maximal IL-1 production and release (Figure 5B). When vehicle versus T0070907 was given to IFNR KO pMACs, IL-1β were the same between the two treatments (Figure 5B). IL-1β levels also increased compared to WT cells indicating that the reduction in IL-1β is dependent on the loss of PPARγ and augmented IFNβ. At the mRNA level, although the IL-1β levels in the KO cells have not completely normalized to WT levels, we see the trend that with the IFNAR antibody present, there is an increase in the IL-1β levels (Figure 5C). This is also seen to be selective since there is no significant difference in TNFα levels with the WT versus the KO cells both treated with the IFNAR antibody and the control IgG (Figure 5C). At the protein level there appears to be little to no difference in the amount of pro-IL-1β levels between the genotypes treated with the IFNAR antibody, and decreases in the amount of pro-IL-1β in the KO compared with the WT when the control IgG was given (Figure 5D). This appears to be selective for IL-1β since there are no differences in the NLRP3 protein with the treatments. Tubulin was used as a loading control.

Figure 5

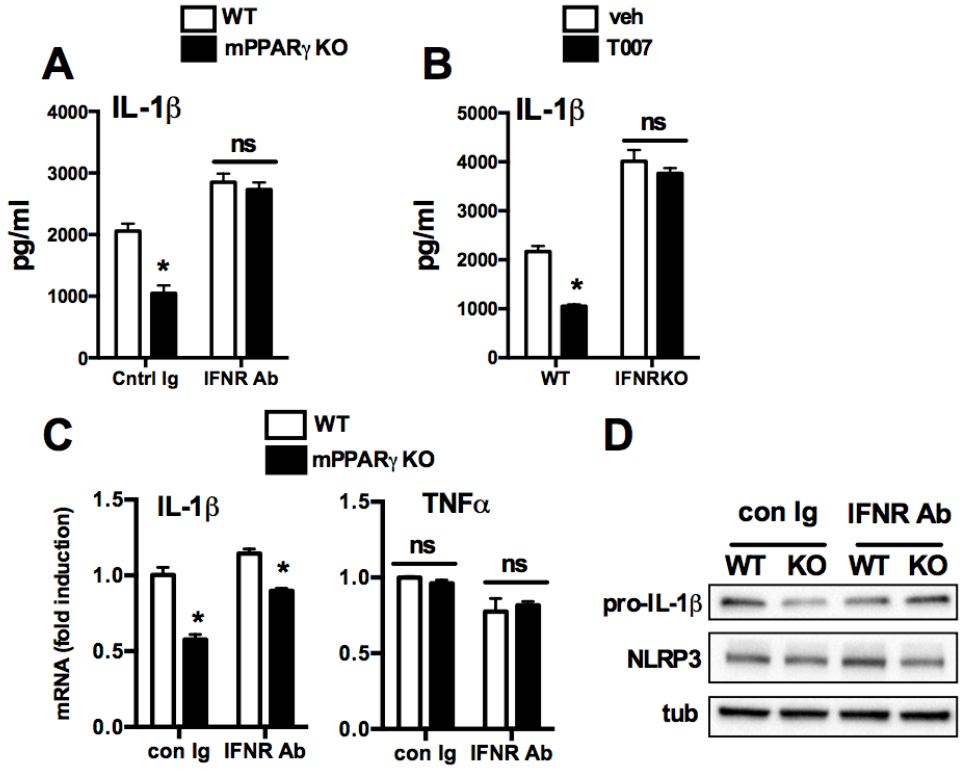

Figure 5. Neutralization of the IFNβ Signal Normalizes IL-1 Levels in Myeloid Specific PPARγ Knock-out Mice. (**A**) WT or PPARγKO pMACs were treated with palm-LPS for 20hrs in the presence of an IFNAR blocking antibody or control Ig and IL-1β release was quantified by ELISA. (**B**) WT or IFNAR KO pMACs were treated with veh or the PPARγ antagonist T0070907 24hrs prior to stimulation with palm-LPS and IL-1β release was quantified by ELISA. (**C, D**) WT or PPARγKO pMACs were treated with palm-LPS for 8hrs (mRNA) or 16hrs (protein) in the presence of an IFNAR blocking antibody or control Ig and IL-1β expression was assessed via qRT-PCR (**C**) and western blotting (**D**). Bar graphs report the mean ± standard error (SE) for a minimum of 3 experiments, each performed in triplicate. *, $p<0.05$ for WT vs. mPPARγKO or; ns, non-significant.

Recombinant IFNβ Sufficient to Reproduce Myeloid Specific PPARγ Knock-out Phenotype

After determining that neutralizing of the IFNβ response was necessary to normalize the IL-1β levels to the WT amount in the mPPARγ KO mice, we wanted to determine if IFNβ was sufficient to recapitulate the KO phenotype. Figure 6A shows that IL-1β release levels were decreased in a dose dependent manner when WT cells were treated with recombinant IFNβ (rIFNβ). TNFα, however, showed no difference in levels when rIFNβ was given exogenously (Figure 6B).

Obvious decreases in pro-IL-1β protein were also seen when rIFNβ was given as well (Figure 6C). Exogenous IFNβ given to WT cells also lead to a decrease in IL-1β mRNA (Figure 6D). Not surprisingly, treatment with rIFNβ also lead to increased CXCL10, which as previously stated is a known IFNβ regulated gene. When rIFNβ was given to WT cells treated with the IFNAR antibody, however, the IL-1β levels were normalized to WT cells not given exogenous IFNβ (Figure 6E). This data phenocopied what was previously seen in the mPPARγ KO cells, giving a strong indication that IFNβ is both necessary and sufficient to cause the phenotype seen.

Figure 6

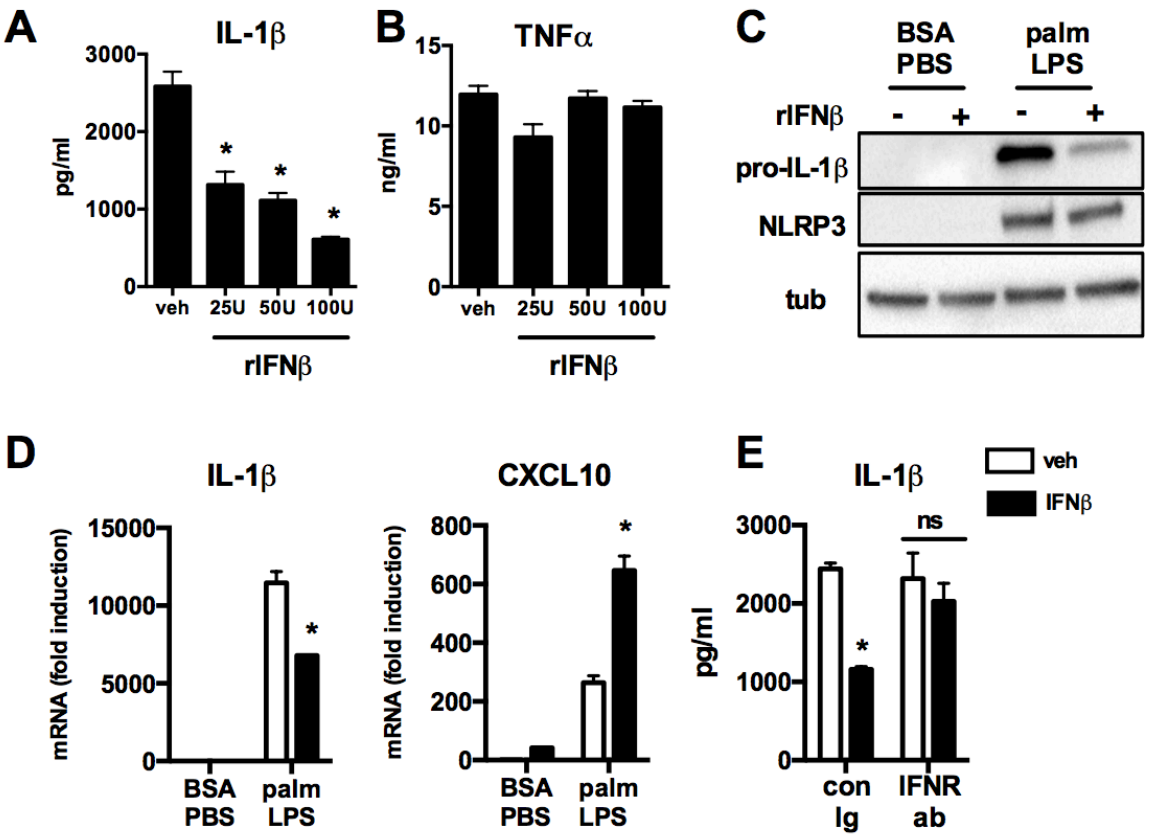

Figure 6. Recombinant IFNβ Sufficient to Reproduce Myeloid Specific PPARγ Knock-out Phenotype. (A, B) WT pMACs were treated with palm-LPS and increasing concentrations of IFNβ after which IL-1β (**A**) and TNFα (**B**) release was quantified by ELISA. (**C**) Macrophages were treated with vehicle or palm-LPS for 16hrs in the presence of IFNβ (50U) and pro-IL-1β and NLRP3 protein levels were assessed by western blotting. Tubulin is shown as a loading control. (**D**) pMACS were treated as indicated and gene expression of IL-1β and CXCL10 was assessed 8hrs after stimulation via qRT-PCR. (**E**) pMACS were stimulated with palm-LPS ± IFNβ in the

presence of IFNAR blocking ab or control Ig and IL-1β release was determined by ELISA. Bar graphs report the mean ± standard error (SE) for a minimum of 3 experiments, each performed in triplicate. *, $p<0.05$ for veh vs. IFNβ or WT vs. IFNAR KO; ns, non-significant.

Agonist of PPARγ Reverses Myeloid Specific PPARγ Knock-out Phenotype

The lab also performed a gain of function model to determine how a heightened PPARγ signal would modulate inflammatory responses and lipid handling in pMACs. Rosiglitazone is a known agonist of PPARγ and a pharmacological agent given as an antidiabetic drug which works to increase insulin sensitivity by binding to PPAR and making cells more responsive to insulin (29). Two different doses of rosiglitazone were given, 1μM which would lead to PPARγ dependent effects, and 10μM which would produce PPARγ independent effects, and likely works to activate other transcription factors such as PPARβ/δ. The pMACs were incubated with 1μM of rosiglitazone for 16 hrs prior to the addition of vehicle or palm-LPS. Not surprisingly, there was an increase in IFNβ and IFN-regulated genes in the mPPARγ KO mice when compared to the WT (Figure 7A-D). As mentioned previously, CXCL10 and MX1 are IFNβ regulated genes. iNOS is a specific isotype of the general enzyme class nitric oxide synthase involved in immune responses, which catalyzes the production of nitric oxide (NO). It is known that PPARγ negatively regulates the expression of iNOS (30). Not surprisingly, iNOS mRNA decreased in a dose dependent manner when WT cells were treated with rosiglitazone. In the KO cells, there was no difference in iNOS mRNA when treated with the low dose rosiglitazone, but when the agonist led to PPARγ independent effects, there was also a reduction in iNOS mRNA (Figure 7D). Figure 7A shows that when WT cells were treated with 1μM rosiglitazone, there was a reduction in the amount of IFNβ present, which is expected since it would augment the effects of PPARγ. As expected, IL-1β mRNA was down in the KO cells compared to WT (Figure 7E). Interestingly, however, the presence of rosiglitazone had little to no effect on IL-1β levels in WT cells (Figure 7E). TNFα expression was unaffected by both loss of PPARγ and augmentation of PPARβ/δ with the addition of rosiglitazone (Figure 7F). To note in all of the panels in Figure 7, there was no significant difference in the KO cells when treated with vehicle or 1μM of rosiglitazone, which is expected since PPARγ is absent from these cells. However, when cells were stimulated with 10μM of rosiglitazone, there began to be PPARγ independent effects as seen in Figure 7B-E. The higher dose of rosiglitazone was shown to suppress IFN-gene expression, and also restore IL-1β levels to baseline WT levels.

Figure 7

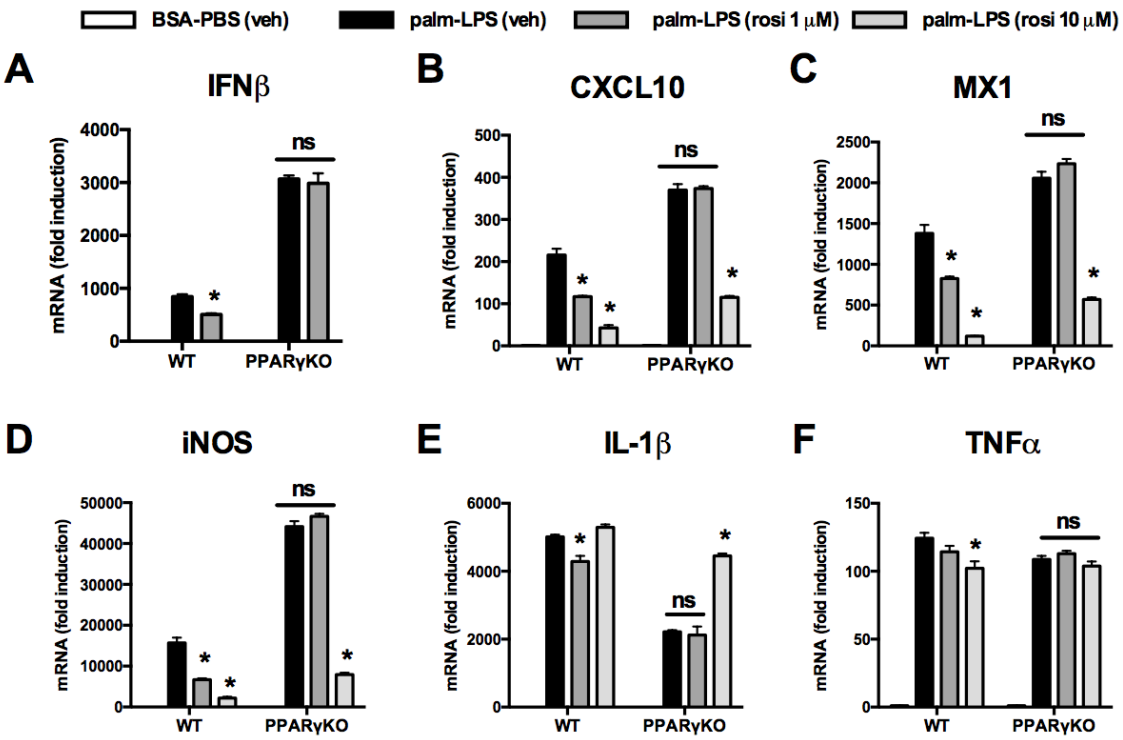

Figure 7. Agonist of PPARγ Reverses Myeloid Specific PPARγ Knock-out Phenotype. (**A-F**) WT or PPARγ KO macrophages were treated with BSA-PBS/veh (open bars), palm-LPS/veh (filled bars), palm-LPS/rosiglitazone 1 μM (dark gray bars) or LPS/rosiglitazone 10 μM (light gray bars) for 16hrs followed by stimulation with palm-LPS for 8hrs (or 1hr in the case of IFNβ) in continued presence of the PPARγ agonist. mRNA was isolated from the macrophages and the expression of IFNβ (**A**) and several of its gene targets (**B-D**) was assessed by qRT-PCR. In addition, mRNA expression of the pro-inflammatory cytokines IL-1β (**E**) and TNFα (**F**) was also determined. Bar graphs report the mean ± standard error (SE) for a minimum of 3 experiments, each performed in triplicate. *, $p<0.05$ for veh vs. rosiglitazone; ns, non-significant.

Discussion

Along with insulin resistant, two hallmarks of T2DM are metabolic stress and inflammation. It has been previously established that metabolic changes that take place can lead to inflammasome activation due to changes in lipid stress and handling (29). A hallmark of T2DM and obesity is a lipid bathed environment which is known to lead to metabolic stress (6, 8, 31). As part of the innate immune system, macrophages play a critical role in regulation of tissue damage and inflammation. It is for this reason our lab studied pMACs to gain insight into the interplay between lipid handling and inflammation. Our lab has previously shown that increased IL-1β is released from macrophages in a high lipid environment, as well as having a critical role in inflammation (6). Finding possible mechanisms of selective reduction of IL-1β would therefore be advantageous therapeutically to reduce the inflammatory response.

In this study, pMACs were stimulated with palmitate and LPS acting as the two signals needed to activate the inflammasome. Palmitate mimics the high lipid environment known to be associated with T2DM and was shown in our lab to lead to lysosome damage (8). LPS acts as the other signal necessary to fully activate the inflammasome and lead to mature IL-1β release. Myeloid specific PPARγ KO pMACs were stimulated with PL showed selective inhibition of IL-1β, but not a global wipe out of the inflammasome, as noted with no changes in TNFα, which is another cytokine known to be released by activated macrophages. PPARγ is a transcription factor, but it is known that it does not directly affect IL-1β transcription by sitting on its promoter (32). Interestingly, the mPPARγ KO cells showed increased IFNβ both through RNA sequencing, and confirmed in our lab with mRNA data on IFN-regulated genes. Furthermore, IFNβ was seen to be both necessary and sufficient to recapitulate the mPPARγ KO cell's phenotype. This was shown by blocking IFNβ through the IFNR antibody, leading to loss of the mPPARγ KO phenotype of decreased IL-1β levels. When WT cells were stimulated and incubated with rIFNβ, there was a selective decrease in IL-1 levels, which is consistent with the mPPARγ KO phenotype. Opposite of the mPPARγ KO model, when we performed a gain of function of PPARγ by the addition of rosiglitazone, a synthetic PPARγ agonist, we saw a decreased IFNβ and IFN-regulated genes signature. This data taken together demonstrates that the augmented IFNβ response was responsible for the selective inhibition of IL-1 levels in macrophages deficient in PPARγ. These results add to the understanding of antagonistic relationship between PPARγ and IFN related inflammatory responses.

Recently published in The New England Journal of Medicine, the CANTOS Trial Group conducted a clinical trial using an IL-1β blocking antibody. Results showed a 26 percent greater reduction in high-sensitivity C-reactive protein and a significantly lower rate of recurrent

cardiovascular events when compared with the placebo. This provides further evidence to the benefits of finding therapeutic agents to selectively inhibit IL-1β to reduce inflammation and metabolic stress. Currently, IFNβ is used as a therapeutically to reduce symptoms of multiple sclerosis (MS) even though it is somewhat unclear as to its mechanism of action. IFNβ is known to suppress T cell activation as well as regulation of pro and anti-inflammatory cytokines (33-36). Both of these treatments provide insight into possible clinically relevant treatments that could possibly come from the data presented in this thesis.

Further investigations will be necessary to determine the mechanism behind which IFNβ is working to selectively inhibit IL-1β levels. Furthermore, it should be established how the loss of PPARγ leads to an increase of IFNβ. One attempt to determine the mechanism of interplay would be to create a PPARγ / IFNβ KO mouse model. Being able to mechanistically establish the connection between PPARγ and IFNβ, and IFNβ and IL-1 would aid in better understanding how to decreases the release of pro-inflammatory cytokines. Also, further research should investigate how agonists of PPARγ could be used therapeutically to suppress IFNβ production, which would be advantageous for patients suffering from autoimmune diseases, since type 1 IFN can promote autoimmunity (37, 38).

In summary, the current study identifies that myeloid specific loss of the transcription factor PPARγ leads to selective reduction of IL-1β via increased IFNβ in peritoneal macrophages. Reduction in IL-1β is via a signal 1 change in the inflammasome complex, as seen by a reduction in pro-IL-1β without reduction in other known inflammasome markers including NLRP3 and TNFα. IFNβ was both necessary and sufficient to reduce IL-1β levels. Macrophage dysfunction is a key component to the pathology of T2DM and obesity. Understanding how the high lipid environment leads to metabolic stress and a pro-inflammatory state. Our data adds to the complexity between inflammation and lipid metabolism, which is known to be at play in prevalent metabolic diseases such as T2DM and obesity.

References

1. Association, A. D. 2018. Statistics About Diabetes: Overall Numbers, Diabetes and Prediabetes. Diabetes.org ed.
2. Prevention, C. f. D. C. a. 2017. Long-term Trends in Diabetes. CDC.gov.
3. HALLGREN, B., S. STENHAGEN, A. SVANBORG, and L. SVENNERHOLM. 1960. Gas chromatographic analysis of the fatty acid composition of the plasma lipids in normal and diabetic subjects. *J Clin Invest* 39: 1424-1434.
4. Laakso, M., M. Suhonen, R. Julkunen, and K. Pyörälä. 1990. Plasma insulin, serum lipids and lipoproteins in gall stone disease in non-insulin dependent diabetic subjects: a case control study. *Gut* 31: 344-347.
5. Schroder, K., R. Zhou, and J. Tschopp. 2010. The NLRP3 inflammasome: a sensor for metabolic danger? *Science* 327: 296-300.
6. Schilling, J. D., H. M. Machkovech, L. He, R. Sidhu, H. Fujiwara, K. Weber, D. S. Ory, and J. E. Schaffer. 2013. Palmitate and lipopolysaccharide trigger synergistic ceramide production in primary macrophages. *J Biol Chem* 288: 2923-2932.
7. Khanna, S., S. Biswas, Y. Shang, E. Collard, A. Azad, C. Kauh, V. Bhasker, G. M. Gordillo, C. K. Sen, and S. Roy. 2010. Macrophage dysfunction impairs resolution of inflammation in the wounds of diabetic mice. *PLoS One* 5: e9539.
8. Weber, K., and J. D. Schilling. 2014. Lysosomes integrate metabolic-inflammatory cross-talk in primary macrophage inflammasome activation. *J Biol Chem* 289: 9158-9171.
9. Tilg, H., A. R. Moschen, and G. Szabo. 2016. Interleukin-1 and inflammasomes in alcoholic liver disease/acute alcoholic hepatitis and nonalcoholic fatty liver disease/nonalcoholic steatohepatitis. *Hepatology* 64: 955-965.
10. Xiao, J., and G. L. Tipoe. 2016. Inflammasomes in non-alcoholic fatty liver disease. *Front Biosci (Landmark Ed)* 21: 683-695.
11. Razani, B., C. Feng, T. Coleman, R. Emanuel, H. Wen, S. Hwang, J. P. Ting, H. W. Virgin, M. B. Kastan, and C. F. Semenkovich. 2012. Autophagy links inflammasomes to atherosclerotic progression. *Cell Metab* 15: 534-544.
12. Duewell, P., H. Kono, K. J. Rayner, C. M. Sirois, G. Vladimer, F. G. Bauernfeind, G. S. Abela, L. Franchi, G. Nuñez, M. Schnurr, T. Espevik, E. Lien, K. A. Fitzgerald, K. L. Rock, K. J. Moore, S. D. Wright, V. Hornung, and E. Latz. 2010. NLRP3 inflammasomes are required for atherogenesis and activated by cholesterol crystals. *Nature* 464: 1357-1361.
13. Lee, H. M., J. J. Kim, H. J. Kim, M. Shong, B. J. Ku, and E. K. Jo. 2013. Upregulated NLRP3 inflammasome activation in patients with type 2 diabetes. *Diabetes* 62: 194-204.
14. Wen, H., D. Gris, Y. Lei, S. Jha, L. Zhang, M. T. Huang, W. J. Brickey, and J. P. Ting. 2011. Fatty acid-induced NLRP3-ASC inflammasome activation interferes with insulin signaling. *Nat Immunol* 12: 408-415.
15. Schilling, J. D., H. M. Machkovech, L. He, A. Diwan, and J. E. Schaffer. 2013. TLR4 activation under lipotoxic conditions leads to synergistic macrophage cell death through a TRIF-dependent pathway. *J Immunol* 190: 1285-1296.

16. Listenberger, L. L., D. S. Ory, and J. E. Schaffer. 2001. Palmitate-induced apoptosis can occur through a ceramide-independent pathway. *J Biol Chem* 276: 14890-14895.
17. Akira, S., and K. Takeda. 2004. Functions of toll-like receptors: lessons from KO mice. *C R Biol* 327: 581-589.
18. Takeda, K., and S. Akira. 2005. Toll-like receptors in innate immunity. *Int Immunol* 17: 1-14.
19. Yamamoto, M., S. Sato, H. Hemmi, K. Hoshino, T. Kaisho, H. Sanjo, O. Takeuchi, M. Sugiyama, M. Okabe, K. Takeda, and S. Akira. 2003. Role of adaptor TRIF in the MyD88-independent toll-like receptor signaling pathway. *Science* 301: 640-643.
20. Zhao, W., L. Wang, M. Zhang, P. Wang, L. Zhang, C. Yuan, J. Qi, Y. Qiao, P. C. Kuo, and C. Gao. 2011. Peroxisome proliferator-activated receptor gamma negatively regulates IFN-beta production in Toll-like receptor (TLR) 3- and TLR4-stimulated macrophages by preventing interferon regulatory factor 3 binding to the IFN-beta promoter. *J Biol Chem* 286: 5519-5528.
21. Vandenbon, A., S. Teraguchi, S. Akira, K. Takeda, and D. M. Standley. 2012. Systems biology approaches to toll-like receptor signaling. *Wiley Interdiscip Rev Syst Biol Med* 4: 497-507.
22. Hevener, A. L., J. M. Olefsky, D. Reichart, M. T. Nguyen, G. Bandyopadyhay, H. Y. Leung, M. J. Watt, C. Benner, M. A. Febbraio, A. K. Nguyen, B. Folian, S. Subramaniam, F. J. Gonzalez, C. K. Glass, and M. Ricote. 2007. Macrophage PPAR gamma is required for normal skeletal muscle and hepatic insulin sensitivity and full antidiabetic effects of thiazolidinediones. *J Clin Invest* 117: 1658-1669.
23. Odegaard, J. I., R. R. Ricardo-Gonzalez, M. H. Goforth, C. R. Morel, V. Subramanian, L. Mukundan, A. Red Eagle, D. Vats, F. Brombacher, A. W. Ferrante, and A. Chawla. 2007. Macrophage-specific PPARgamma controls alternative activation and improves insulin resistance. *Nature* 447: 1116-1120.
24. Weber, K. J., M. A. Sauer, L. He, G. Kalugotla, B. Razani, and J. D. Schilling. Suppression of IL-1 in PPARg Deficient Macrophages occurs via type 1 interferon Dependent Mechanism. Manuscript under review.
25. He, L., K. J. Weber, and J. D. Schilling. 2016. Glutamine Modulates Macrophage Lipotoxicity. *Nutrients* 8: 215.
26. Sharma, A., M. Tate, G. Mathew, J. E. Vince, R. H. Ritchie, and J. B. de Haan. 2018. Oxidative Stress and NLRP3-Inflammasome Activity as Significant Drivers of Diabetic Cardiovascular Complications: Therapeutic Implications. *Front Physiol* 9: 114.
27. Petry, H., L. Cashion, P. Szymanski, O. Ast, A. Orme, C. Gross, M. Bauzon, A. Brooks, C. Schaefer, H. Gibson, H. Qian, G. M. Rubanyi, and R. N. Harkins. 2006. Mx1 and IP-10: biomarkers to measure IFN-beta activity in mice following gene-based delivery. *J Interferon Cytokine Res* 26: 699-705.
28. Gil, M. P., M. J. Ploquin, W. T. Watford, S. H. Lee, K. Kim, X. Wang, Y. Kanno, J. J. O'Shea, and C. A. Biron. 2012. Regulating type 1 IFN effects in CD8 T cells during viral infections: changing STAT4 and STAT1 expression for function. *Blood* 120: 3718-3728.

29. Eguchi, A., M. Lazic, A. M. Armando, S. A. Phillips, R. Katebian, S. Maraka, O. Quehenberger, D. D. Sears, and A. E. Feldstein. 2016. Circulating adipocyte-derived extracellular vesicles are novel markers of metabolic stress. *J Mol Med (Berl)* 94: 1241-1253.
30. Pascual, G., A. L. Fong, S. Ogawa, A. Gamliel, A. C. Li, V. Perissi, D. W. Rose, T. M. Willson, M. G. Rosenfeld, and C. K. Glass. 2005. A SUMOylation-dependent pathway mediates transrepression of inflammatory response genes by PPAR-gamma. *Nature* 437: 759-763.
31. Cascio, G., G. Schiera, and I. Di Liegro. 2012. Dietary Fatty Acids in Metabolic Syndrome, Diabetes and Cardiovascular Diseases. Bentham Science. 2-17.
32. Ghisletti, S., W. Huang, S. Ogawa, G. Pascual, M. E. Lin, T. M. Willson, M. G. Rosenfeld, and C. K. Glass. 2007. Parallel SUMOylation-dependent pathways mediate gene- and signal-specific transrepression by LXRs and PPARgamma. *Mol Cell* 25: 57-70.
33. Haji Abdolvahab, M., M. R. Mofrad, and H. Schellekens. 2016. Interferon Beta: From Molecular Level to Therapeutic Effects. *Int Rev Cell Mol Biol* 326: 343-372.
34. Airas, L., J. Niemelä, G. Yegutkin, and S. Jalkanen. 2007. Mechanism of action of IFN-beta in the treatment of multiple sclerosis: a special reference to CD73 and adenosine. *Ann N Y Acad Sci* 1110: 641-648.
35. Guo, S., D. Bozkaya, A. Ward, J. A. O'Brien, K. Ishak, R. Bennett, A. Al-Sabbagh, and D. M. Meletiche. 2009. Treating relapsing multiple sclerosis with subcutaneous versus intramuscular interferon-beta-1a: modelling the clinical and economic implications. *Pharmacoeconomics* 27: 39-53.
36. Jakimovski, D., C. Kolb, M. Ramanathan, R. Zivadinov, and B. Weinstock-Guttman. 2018. Interferon β for Multiple Sclerosis. *Cold Spring Harb Perspect Med*.
37. Chasset, F., and L. Arnaud. 2018. Targeting interferons and their pathways in systemic lupus erythematosus. *Autoimmun Rev* 17: 44-52.
38. Kim, H., G. A. Sanchez, and R. Goldbach-Mansky. 2016. Insights from Mendelian Interferonopathies: Comparison of CANDLE, SAVI with AGS, Monogenic Lupus. *J Mol Med (Berl)* 94: 1111-1127.